GEOLOGY | THE GEOLOGICAL SOCIETY OF AMERICA®

https://doi.org/10.1130/G50842.1

Manuscript received 12 October 2022
Revised manuscript received 13 January 2023
Manuscript accepted 14 January 2023

Published online 15 March 2023

The early opening of the Equatorial Atlantic gateway and the evolution of Cretaceous peak warming

Wolf Dummann[1,2]*, Peter Hofmann[2], Jens O. Herrle[1], Martin Frank[3] and Thomas Wagner[4]
[1]Institute of Geosciences, Goethe-University Frankfurt, 60438 Frankfurt am Main, Germany
[2]Institute of Geology and Mineralogy, University of Cologne, 50674 Cologne, Germany
[3]GEOMAR Helmholtz Centre for Ocean Research Kiel, 24148 Kiel, Germany
[4]Lyell Centre, School of Energy, Geoscience, Infrastructure and Society, Heriot-Watt University, Edinburgh EH14 4AS, UK

ABSTRACT

The Cretaceous opening of the Equatorial Atlantic gateway (EAG) is considered a driver of major changes in global oceanography, carbon cycling, and climate. However, the early stages of EAG opening are poorly understood. We present seawater Nd-isotope, bulk geochemical, and micropaleontological data from two South Atlantic drill cores that constrain the onset of shallow (<500 m) and intermediate (<~1000 m) water mass exchange across the EAG to 113 Ma and 107 Ma, respectively. Deep water mass exchange (>2000 m) was enabled by at least ca. 100 Ma, as much as 10 m.y. earlier than previously estimated. In response to EAG opening, deep-water ventilation in the South Atlantic, North Atlantic, and Tethys basins intensified, thereby triggering basin-scale reductions in organic carbon burial. We propose that the consequent drop in carbon sequestration in concert with increased atmospheric CO_2 fluxes from subduction zones acted as major amplifiers of global warming that culminated in peak greenhouse conditions during the mid-Cretaceous.

INTRODUCTION

The mid-Cretaceous (i.e., ca. 120–90 Ma) opening of the Equatorial Atlantic gateway (EAG) induced a major reorganization of global ocean circulation patterns with important repercussions on deep ocean oxygenation, carbon cycling, and climate (e.g., Poulsen et al., 2003). In particular, the onset or intensification of deep water mass exchange across the EAG from Turonian time onward has been linked to global climate cooling and the transition to better-ventilated deep oceans (Robinson et al., 2010; Friedrich et al., 2012). In contrast, little is known about the pre-Turonian evolution of the EAG. A growing body of paleobiogeographic (e.g., Bruno et al., 2020; Luft-Souza et al., 2022) and sedimentological (e.g., Wagner and Pletsch, 1999; Behrooz et al., 2018) evidence, however, suggests an earlier (i.e., ca. 115–100 Ma) onset of significant water mass exchange across the EAG, yet the exact timing of the onset, extent, and depth of water mass exchange are poorly resolved. An early opening of the EAG at a time when Cretaceous greenhouse climate was approaching its climax (e.g., O'Brien et al., 2017) would imply yet-unexplored linkages between the EAG opening and global climate.

We constrain the relative timing of changes in tectonics, ocean circulation, and climate in response to the EAG opening based on new Aptian to Cenomanian shallow- and intermediate-water Nd-isotope records from two South Atlantic drill sites, which are integrated into an improved stratigraphic framework.

GEOLOGICAL SETTING

The opening of the South Atlantic Basin started at ca. 140 Ma and progressed from south to north (Heine et al., 2013). By ca. 120 Ma, rifting had begun north of the Walvis Ridge (Fig. 1B), and extensive evaporites were deposited in the northern South Atlantic. Post-evaporite deposition started during the late Aptian (ca. 119 Ma; Sanjinés et al., 2022), when surface-water exchange with the North Atlantic and/or the southern South Atlantic commenced (Fig. 1B; Bruno et al., 2020; Luft-Souza et al., 2022; Cui et al., 2023). Paleogeographic reconstructions indicate that the final break-up between South America and Africa occurred between ca. 104 and 99 Ma (Heine et al., 2013; Granot and Dyment, 2015). However, it has been suggested that deep-water passages across the EAG did not develop until the Turonian, given that the emerging equatorial Atlantic likely consisted of a series of pull-apart basins with limited connectivity (Wagner and Pletsch, 1999; Pérez-Díaz and Eagles, 2017).

MATERIAL AND METHODS

We present total organic carbon (TOC), total inorganic carbon, and seawater Nd-isotope signatures from Aptian to lower Cenomanian sediments of Deep Sea Drilling Project (DSDP) Sites 363 and 364, located on the Walvis Ridge and in the Kwanza Basin, respectively (Fig. 1). New calcareous nannofossil data and stable carbon isotope ratios of bulk carbonate ($\delta^{13}C_{carb}$) are provided for DSDP Site 363. Seawater Nd-isotope signatures were extracted from sedimentary Fe-Mn-oxyhydroxides following Blaser et al. (2016). Age models for both sites were constructed based on published (Bruno et al., 2020) and new nannofossil biostratigraphic data and corroborated by $\delta^{13}C$ stratigraphy. Details on the analytical methods and age models are available in the Supplemental Material[1].

Basal sediments of DSDP Site 364 were cored a few tens of meters above the underlying evaporites and consist mainly of dolomite and black shale, deposited at neritic water depths under euxinic and hypersaline conditions (Kochhann et al., 2014; Behrooz et al., 2018). During the Albian, the black shales were replaced by limestone, which was accompanied by deepening to bathyal water depths (Kochhann et al., 2014).

*E-mail: dummann@em.uni-frankfurt.de

[1]Supplemental Material. Analytical methods, data quality, and age models, as well as geochemical data. Please visit https://doi.org/10.1130/GEOL.S.22151930 to access the supplemental material, and contact editing@geosociety.org with any questions.

CITATION: Dummann, W., et al., 2023, The early opening of the Equatorial Atlantic gateway and the evolution of Cretaceous peak warming: Geology, v. 51, p. 476–480, https://doi.org/10.1130/G50842.1

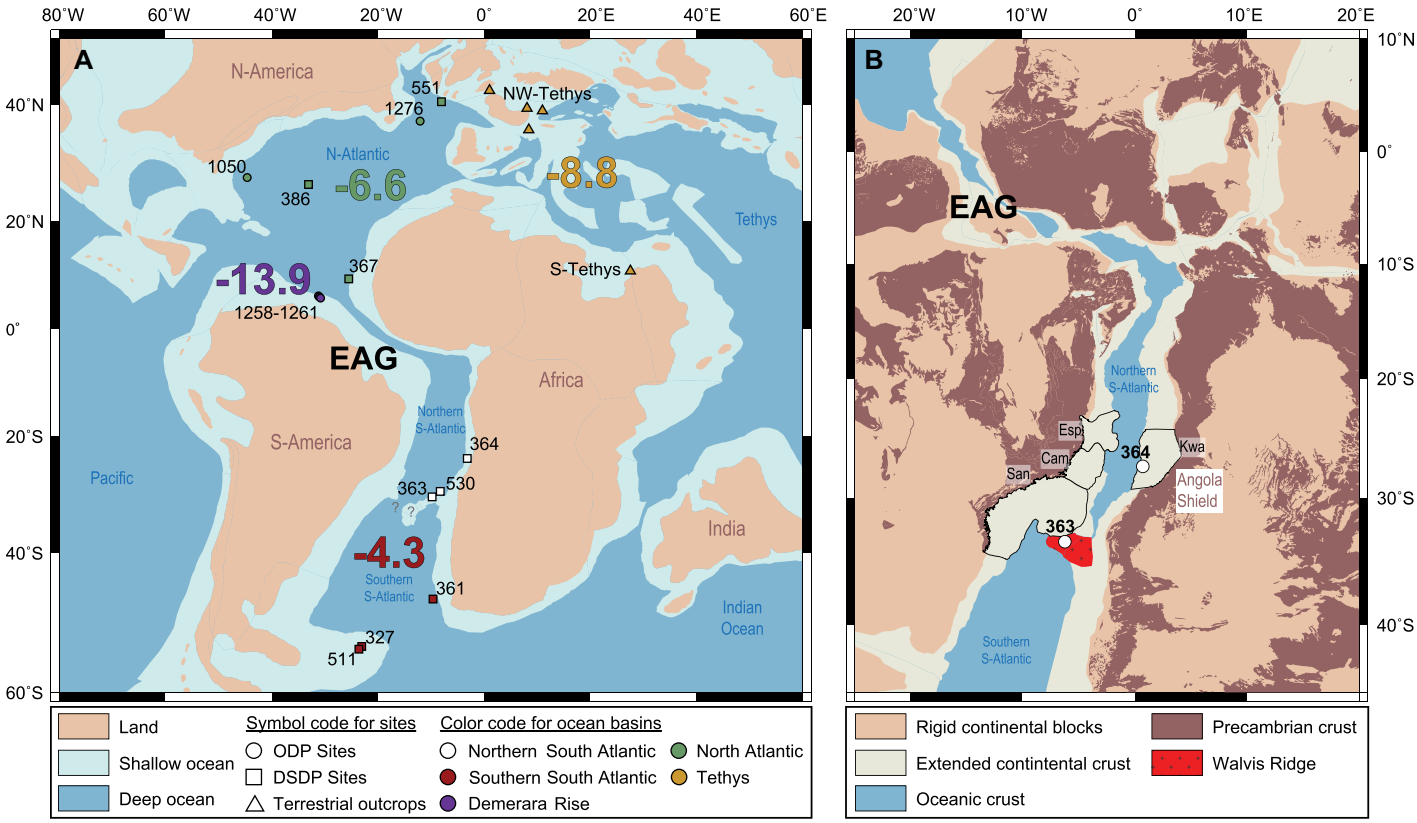

Figure 1. (A) Cenomanian paleogeography (Cao et al., 2017). Colored numbers indicate the average seawater ε_{Nd} for each basin. (B) Paleogeography of the South Atlantic at 112 Ma, including major rift basins (Heine et al., 2013). EAG—Equatorial Atlantic gateway; Kwa—Kwanza Basin; San—Santos Basin; Cam—Campos Basin; Esp—Espirito Santo Basin; DSDP—Deep Sea Drilling Project; ODP—Ocean Drilling Program.

DSDP Site 363 was drilled close to the northeastern crest of the Walvis Ridge and penetrated a sequence of limestone and marl deposited at shallow water depths <500 m (Holbourn et al., 2001).

RESULTS

Seawater ε_{Nd} signatures at DSDP Sites 363 and 364 exhibit long-term (>1 m.y.) patterns (Fig. 2) that are persistent across lithological boundaries (i.e., limestone-marl alternations and shale-dolomite alternations; see the Supplemental Material). Combined with changes in lithology and biotic events, the ε_{Nd} patterns are used to define three stratigraphic phases (Fig. 2), each representing a distinct stage in the oceanographic evolution of the northern South Atlantic. Phase 1 encompasses Aptian dolomite and black shale of DSDP Site 364, which recorded highly unradiogenic ε_{Nd} signatures below −13. The basal age of phase 1 in DSDP Site 364 is poorly constrained due to the lack of diagnostic fossils. A maximum age of 119 Ma can, however, be assigned based on the assumption that post-evaporite sedimentation commenced contemporaneously in the Kwanza Basin and the conjugate Campos, Santos, and Espirito Santo Basins (Fig. 1B), for which more detailed stratigraphic information is available (e.g., Sanjinés et al., 2022). At the base of phase 2, calcareous nannofossils and salinity-tolerant foraminifera first occurred in the Kwanza Basin (Kochhann et al., 2013; Bruno et al., 2020), including *Prediscosphaera columnata* indicative of an early Albian age (younger than ca. 113 Ma). Across phase 2, ε_{Nd} signatures at DSDP Site 364 increased from below −13 to above −9, while more radiogenic and less variable ε_{Nd} signatures between −7.5 and −5.5 were recorded at DSDP Site 363. Above the base of phase 3, organic carbon (OC)–poor limestone dominates at DSDP Site 364 and ε_{Nd} signatures remain overall constant above −9, while DSDP Site 363 recorded a low variability of ε_{Nd} signatures between −6.9 and −6.1. At both sites, the base of phase 3 is located within a few meters above the first occurrence of *Eiffellithus monechiae* (ca. 107.6 Ma). DSDP Site 364 recorded a series of three positive ε_{Nd} excursions, which occurred during all three phases, reached values above −6, and spanned short periods of time (<1 m.y.; Fig. 2).

DISCUSSION

Gateway Evolution and Long-Term Changes in Water Mass Mixing

Aptian post-evaporite sedimentation (phase 1) in the Kwanza Basin occurred under hypersaline and anoxic to euxinic conditions (Behrooz et al., 2018). These oceanographic conditions have been attributed to hydrographic isolation of the northern South Atlantic caused by limited water mass inflow from the south and the north. Aptian ε_{Nd} signatures at DSDP Site 364 were highly unradiogenic and similar to those observed in modern surface waters off Angola (Fig. 2), which obtain their unradiogenic ε_{Nd} signature from local weathering inputs of Precambrian crust exposed along the West African margin (Fig. 1B; Rahlf et al., 2020). Similar rocks were probably weathered during the mid-Cretaceous given that unradiogenic ε_{Nd} signatures of ~−17 have also been reported for Cenomanian shelf waters along the Angola margin (Fig. 2; Grandjean et al., 1987). We therefore propose that Aptian water masses in the northern South Atlantic acquired their ε_{Nd} signatures primarily from local African weathering inputs and were largely isolated from the more radiogenic water masses in the southern South Atlantic (~−4.3; Fig. 2), the North Atlantic (~−6.6), and the Tethys (~−8.8). This pattern implies that the EAG was closed in the Aptian.

From 113 Ma onward, more oxic conditions developed in the Kwanza Basin (Behrooz et al., 2018) and calcareous plankton proliferated implying a change to normal marine salinity (Fig. 2; Kochhann et al., 2013; Bruno et al., 2020). ε_{Nd} signatures at DSDP Site 364 started to increase at the same time (Fig. 2), suggesting

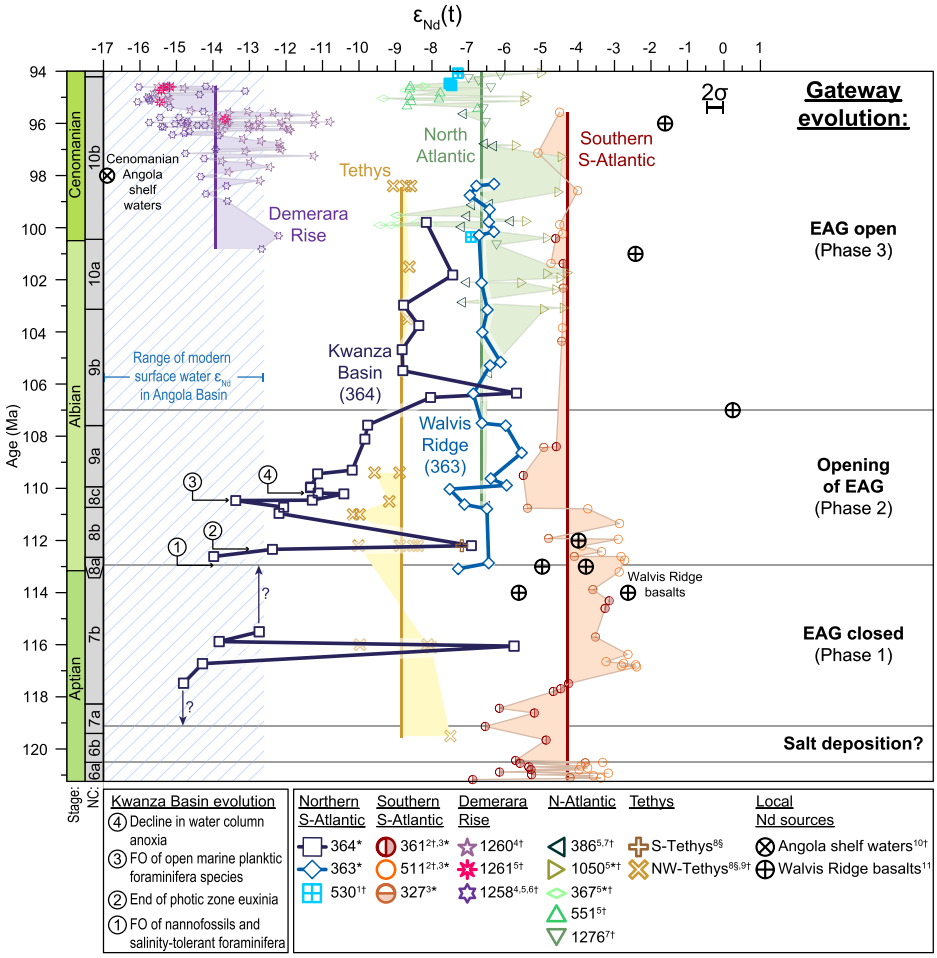

Figure 2. Aptian to Cenomanian ε_{Nd} data, including new data from Deep Sea Drilling Project Sites 363 and 364. NC nannofossil zonation of Bralower (1995) is shown on the left. Thick vertical lines indicate average values for each ocean basin prior to 94.6 Ma (i.e., prior to the onset of oceanic anoxic event 2). For site locations, see Figure 1A. Note that reference sites are located at variable paleo–water depths generally >1000 m. Age models and ε_{Nd}(t) values of all reference sites were updated (see the Supplemental Material [see footnote 1]). Data sources: [1]Robinson et al. (2010); [2]Murphy and Thomas (2013); [3]Dummann et al. (2020); [4]Jiménez Berrocoso et al. (2010); [5]Martin et al. (2012); [6]MacLeod et al. (2008); [7]Robinson and Vance (2012); [8]Soudry et al. (2006); [9]Pucéat et al. (2005); [10]Grandjean et al. (1987); [11]Hoernle et al. (2015). Archives used: *Fe-Mn oxyhydroxides; †fish debris; §authigenic carbonate fluorapatite. EAG—Equatorial Atlantic gateway; FO—first occurrence.

enhanced advection of more radiogenic water masses into the northern South Atlantic. The direction of inflow has been debated (e.g., Cui et al., 2023), but strong Tethyan affinities of plankton in the Kwanza Basin (Kochhann et al., 2013; Bruno et al., 2020) and basins along the Brazilian margin (Luft-Souza et al., 2022; Sanjinés et al., 2022) support the existence of surface-water connections with the North Atlantic via the emerging EAG. Nannofossil assemblages at DSDP Site 363 also document a Tethyan low- to mid-latitude affinity (see the Supplemental Material), indicating that surface waters entering the northern South Atlantic from the north were advected as far south as the Walvis Ridge. ε_{Nd} signatures of ~−6.5 at DSDP Site 363 overlap with those recorded in the North Atlantic (~−6.6; Fig. 2) but differ markedly from the more radiogenic ε_{Nd} signatures of water masses in the southern South Atlantic (~−4.3) and Walvis Ridge basalts (>−5.6). This pattern is consistent with a predominant inflow from the north, minor (if any) inflow from the south, and little (if any) influence of local Nd contributions from Walvis Ridge basalts. These observations support that shallow connections (<500 m) across the EAG existed at ca. 113 Ma, which gradually widened and/or deepened between 113 and 107 Ma, causing an intensification of water mass exchange with the North Atlantic. We note, however, that the available North Atlantic ε_{Nd} records reflect water masses at depths >1000 m. Given the lack of reference data from shallower depths, we assume a similar ε_{Nd} signature for shallow water masses penetrating the northern South Atlantic (<500 m), implying that water mass properties in the North Atlantic were vertically uniform with respect to ε_{Nd}.

During phase 3, ε_{Nd} signatures at DSDP Sites 363 and 364 remained essentially constant, suggesting persistent circulation patterns at shallow and bathyal water depths, respectively. We suggest that these conditions mark the opening of the EAG to bathyal water depths, which allowed unrestricted inflow of intermediate water masses (<~1000 m) from the north. Contrasting ε_{Nd} signatures persisted between the northern and southern South Atlantic, suggesting limited or absent water mass exchange across the Walvis Ridge and implying tectonically restricted deep-water communication between the North Atlantic and southern high latitudes until at least early Cenomanian times. ε_{Nd} signatures at DSDP Site 364 are offset by 2 ε_{Nd} units to more negative values compared to DSDP Site 363 (Fig. 2), which is likely caused by addition of weathering-derived Nd from West Africa, masking the North Atlantic–derived water mass ε_{Nd} signal. A similar process occurs today in the Angola Basin, where Nd originating from continental weathering and contained in particulate Fe-Mn-oxyhydroxides is supplied to the surface waters. These phases sink and release the Nd at depth, resulting in shifts of local deep-water ε_{Nd} to less radiogenic values by 1–2.5 ε_{Nd} units (Rahlf et al., 2020).

Determining the exact timing of deep-water (>1000 m) mass exchange across the EAG is complicated by the lack of pre-Cenomanian strata at DSDP Site 530, which is located at abyssal depths (>2000 m) in the Angola Basin (Fig. 1A). However, the earliest Cenomanian ε_{Nd} signatures at DSDP Site 530 are indistinguishable from those in the North Atlantic (Fig. 2), suggesting that deep-water connections across the EAG existed from at least ca. 100 Ma onwards, as much as 10 m.y. earlier than indicated by paleobathymetric reconstructions (Pérez-Díaz and Eagles, 2017). This discrepancy in timing could reflect earlier connectivity of sub-basins in the equatorial Atlantic and/or temporal uncertainties in paleobathymetric models.

Short-Term Shifts in ε_{Nd} in the Kwanza Basin

Three positive ε_{Nd} excursions occur randomly distributed and without apparent sedimentary changes in the record of DSDP Site 364 (Fig. 2). By analogy with previous studies of DSDP Site 530 (Murphy and Thomas, 2013), we speculate that the ε_{Nd} excursions reflect the transient input of radiogenic Nd from the dissolution of volcanic ash, potentially ejected at Walvis Ridge during brief episodes of active volcanism.

Implications for Deep Ocean Ventilation and Carbon Cycling

The gradual opening of the EAG coincided with major changes in deep ocean ventilation on a regional to supraregional scale, affecting local and probably also global carbon cycling.

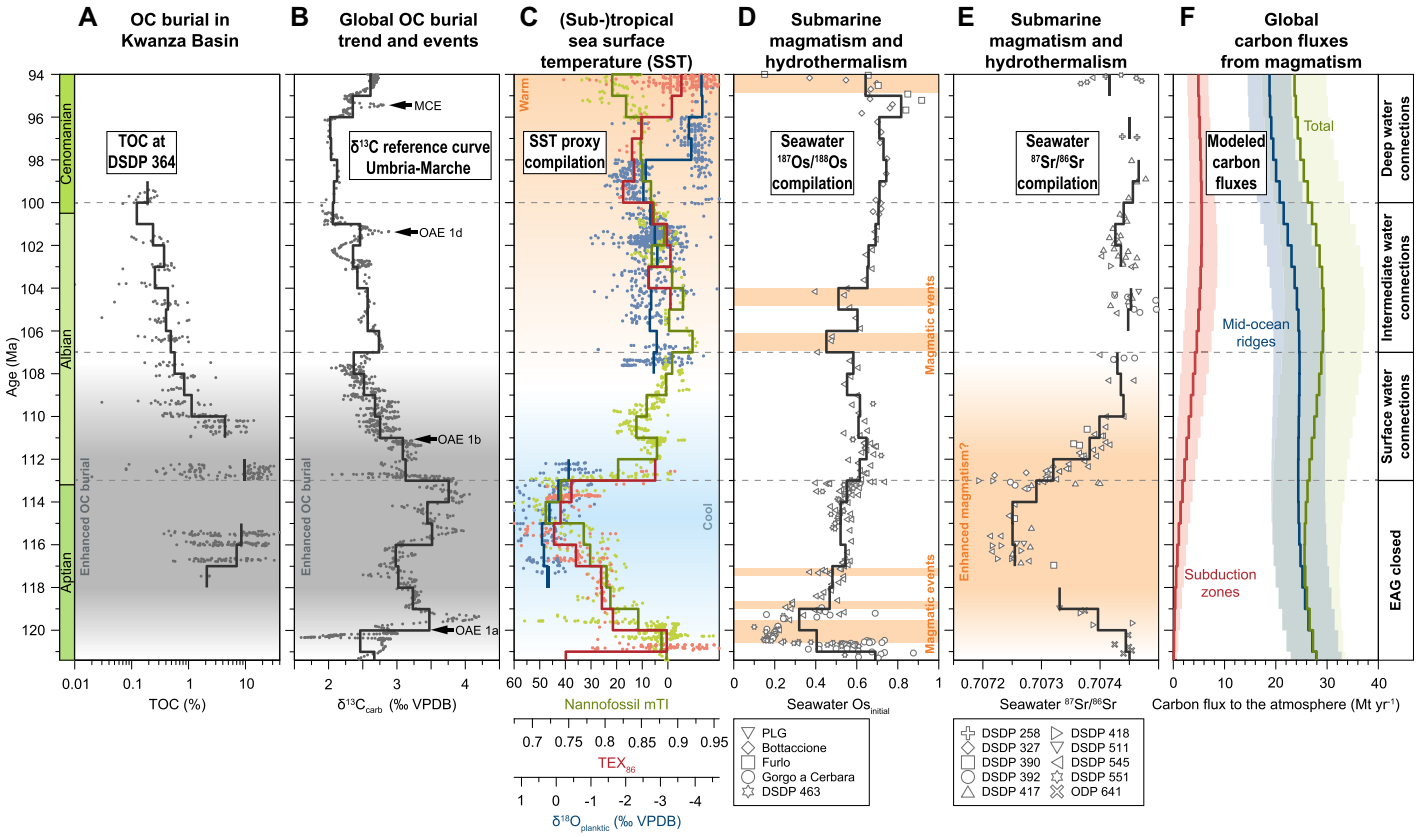

Figure 3. (A) Total organic carbon (TOC) content at Deep Sea Drilling Project (DSDP) Site 364 (Behrooz et al., 2018; this study). (B) Reference stable carbon isotope record from the Umbria-Marche Basin, Italy (Bottini and Erba, 2018). (C) Compiled sea-surface temperature (SST) data between 50°N and 50°S: Modified nannofossil temperature index (mTI) is in green (Bottini and Erba, 2018), TEX_{86} thermometry is in red, and stable oxygen isotope ratios of planktic foraminifera ($\delta^{18}O_{planktic}$) is in blue (O'Brien et al., 2017). (D) Seawater $^{187}Os/^{188}Os$ compilation, including data from the Poggio le Guaine (PLG) core, the Bottaccione, Furlo, and Gorgo a Cerbara sections, and Deep Sea Drilling Project Site 463 (Matsumoto et al., 2022). (E) Seawater $^{87}Sr/^{86}Sr$ compilation (Bralower et al., 1997). (F) Modeled carbon outgassing at subduction zones and mid-ocean ridges (Müller et al., 2022). All step plots represent 1 m.y. averages. EAG—Equatorial Atlantic gateway; MCE—Mid-Cenomanian Event; OAE—oceanic anoxic event; OC—organic carbon; ODP—Ocean Drilling Program; VPDB—Vienna Peedee belemnite.

On a regional scale, enhanced ventilation of deep waters caused a transition from euxinic to oxic conditions in the Kwanza Basin (Behrooz et al., 2018). In concert with this redox shift, TOC contents at DSDP Site 364 decreased by about two orders of magnitude (Fig. 3A), suggesting a major drop in OC burial rates.

Major facies changes from OC-rich sediments to chalk also occurred in the Tethys and northern North Atlantic between ca. 104 and 100 Ma, suggesting intensification of deep-water ventilation also on a supraregional scale (Giorgioni et al., 2015). Consistent with general circulation model results (Poulsen et al., 2003), we consider this ventilation change to be a far-field effect of the EAG opening. By ca. 113 Ma, OC burial rates in the southern South Atlantic also decreased, albeit related to the opening of southern South Atlantic–Southern Ocean gateways (Dummann et al., 2020). These results imply changes in carbon cycling in at least three of the major ocean basins, which had acted as important depocenters of OC and cumulatively contributed 30% to total global OC burial (McAnena et al., 2013). We hypothesize that reduced OC burial in these basins may have caused, or at least contributed to, changes in the global carbon cycle that are reflected in a concurrent global decline in $\delta^{13}C$ values (Fig. 3B).

Implications for Cretaceous Climate

The Albian marked a turning point in the evolution of Cretaceous climate, heralding a period of global warming that culminated in extreme greenhouse conditions during the Turonian (Fig. 3C; O'Brien et al., 2017; Bottini and Erba, 2018). The mechanisms that triggered peak greenhouse conditions are controversial, with mounting evidence questioning the importance of magmatism (e.g., Matsumoto et al., 2022), which is widely considered to be the main cause of warming. In particular, there are long-term increases in seawater $^{187}Os/^{188}Os$ and $^{87}Sr/^{86}Sr$ ratios across the warming interval, suggesting reduced submarine magmatism and hydrothermal activity (Figs. 3D and 3E; Bralower et al., 1997; Matsumoto et al., 2022). Thermodynamic modeling likewise indicates reduced CO_2 outgassing from mid-ocean ridges (Fig. 3F; see the Supplemental Material; Müller et al., 2022). However, carbon fluxes from subduction zones increased (Fig. 3F). Although minor in comparison to the carbon flux from mid-ocean ridges, injection of carbon from subduction-related volcanism directly into the atmosphere may have had greater potential to influence climate trends than submarine volcanism (Matsumoto et al., 2022). We therefore propose that the disappearance of oceanic carbon sinks in the South Atlantic, North Atlantic, and Tethys basins induced by the opening of the EAG and southern South Atlantic–Southern Ocean gateways, combined with enhanced CO_2 fluxes from subduction volcanism (Fig. 3F), was instrumental in driving the Cretaceous climate toward peak warming.

ACKNOWLEDGMENTS

This research used samples provided by the Deep Sea Drilling Project (DSDP) and was funded by German Research Foundation grants to Hofmann and Herrle (grants HO2188/9 and HE3521/9-2). Cinzia Bottini, Elisabetta Erba, and Hironao Matsumoto are thanked for providing reference data. We thank Stuart Robinson and two anonymous reviewers for their valuable comments and suggestions.

REFERENCES CITED

Behrooz, L., Naafs, B.D.A., Dickson, A.J., Love, G.D., Batenburg, S.J., and Pancost, R.D., 2018,

Astronomically driven variations in depositional environments in the South Atlantic during the Early Cretaceous: Paleoceanography and Paleoclimatology, v. 33, p. 894–912, https://doi.org/10.1029/2018PA003338.

Blaser, P., Lippold, J., Gutjahr, M., Frank, N., Link, J.M., and Frank, M., 2016, Extracting foraminiferal seawater Nd isotope signatures from bulk deep sea sediment by chemical leaching: Chemical Geology, v. 439, p. 189–204, https://doi.org/10.1016/j.chemgeo.2016.06.024.

Bottini, C., and Erba, E., 2018, Mid-Cretaceous paleoenvironmental changes in the western Tethys: Climate of the Past, v. 14, p. 1147–1163, https://doi.org/10.5194/cp-14-1147-2018.

Bralower, T.J., Leckie, R.M., Sliter, W.V., and Thierstein, H.R., 1995, An integrated Cretaceous microfossil biostratigraphy, *in* Berggren, W.A., et al., eds., Geochronology, Time Scales and Global Stratigraphic Correlations; SEPM Special Publication 54, p. 65–79.

Bralower, T.J., Fullagar, P.D., Paull, C.K., Dwyer, G.S., and Leckie, R.M., 1997, Mid-Cretaceous strontium-isotope stratigraphy of deep-sea sections: Geological Society of America Bulletin, v. 109, p. 1421–1442, https://doi.org/10.1130/0016-7606(1997)109<1421:MCSISO>2.3.CO;2.

Bruno, M.D.R., Fauth, G., Watkins, D.K., and Savian, J.F., 2020, Albian–Cenomanian calcareous nannofossils from DSDP Site 364 (Kwanza Basin, Angola): Biostratigraphic implications for the South Atlantic: Cretaceous Research, v. 109, 104377, https://doi.org/10.1016/j.cretres.2020.104377.

Cao, W.C., Zahirovic, S., Flament, N., Williams, S., Golonka, J., and Müller, R.D., 2017, Improving global paleogeography since the late Paleozoic using paleobiology: Biogeosciences, v. 14, p. 5425–5439, https://doi.org/10.5194/bg-14-5425-2017.

Cui, X.Q., Wignall, B., Freeman, K.H., and Summons, R.E., 2023, Early Cretaceous marine incursions into South Atlantic rift basins originated from the south: Communications Earth & Environment, v. 4, 6, https://doi.org/10.1038/s43247-022-00668-3.

Dummann, W., Steinig, S., Hofmann, P., Flögel, S., Osborne, A.H., Frank, M., Herrle, J.O., Bretschneider, L., Sheward, R.M., and Wagner, T., 2020, The impact of Early Cretaceous gateway evolution on ocean circulation and organic carbon burial in the emerging South Atlantic and Southern Ocean basins: Earth and Planetary Science Letters, v. 530, 115890, https://doi.org/10.1016/j.epsl.2019.115890.

Friedrich, O., Norris, R.D., and Erbacher, J., 2012, Evolution of middle to Late Cretaceous oceans—A 55 m.y. record of Earth's temperature and carbon cycle: Geology, v. 40, p. 107–110, https://doi.org/10.1130/G32701.1.

Giorgioni, M., Weissert, H., Bernasconi, S.M., Hochuli, P.A., Keller, C.E., Coccioni, R., Petrizzo, M.R., Lukeneder, A., and Garcia, T.I., 2015, Paleoceanographic changes during the Albian–Cenomanian in the Tethys and North Atlantic and the onset of the Cretaceous chalk: Global and Planetary Change, v. 126, p. 46–61, https://doi.org/10.1016/j.gloplacha.2015.01.005.

Grandjean, P., Cappetta, H., Michard, A., and Albarède, F., 1987, The assessment of REE patterns and $^{143}Nd/^{144}Nd$ ratios in fish remains: Earth and Planetary Science Letters, v. 84, p. 181–196, https://doi.org/10.1016/0012-821X(87)90084-7.

Granot, R., and Dyment, J., 2015, The Cretaceous opening of the South Atlantic Ocean: Earth and Planetary Science Letters, v. 414, p. 156–163, https://doi.org/10.1016/j.epsl.2015.01.015.

Heine, C., Zoethout, J., and Müller, R.D., 2013, Kinematics of the South Atlantic rift: Solid Earth, v. 4, p. 215–253, https://doi.org/10.5194/se-4-215-2013.

Hoernle, K., Rohde, J., Hauff, F., Garbe-Schönberg, D., Homrighausen, S., Werner, R., and Morgan, J.P., 2015, How and when plume zonation appeared during the 132 Myr evolution of the Tristan Hotspot: Nature Communications, v. 6, https://doi.org/10.1038/ncomms8799.

Holbourn, A., Kuhnt, W., and Soeding, E., 2001, Atlantic paleobathymetry, paleoproductivity and paleocirculation in the late Albian: The benthic foraminiferal record: Palaeogeography, Palaeoclimatology, Palaeoecology, v. 170, p. 171–196, https://doi.org/10.1016/S0031-0182(01)00223-1.

Jiménez Berrocoso, Á., MacLeod, K.G., Martin, E.E., Bourbon, E., Londoño, C.I., and Basak, C., 2010, Nutrient trap for Late Cretaceous organic-rich black shales in the tropical North Atlantic: Geology, v. 38, p. 1111–1114, https://doi.org/10.1130/G31195.1.

Kochhann, K.G.D., Koutsoukos, E.A.M., Fauth, G., and Sial, A.N., 2013, Aptian–Albian planktic foraminifera from DSDP Site 364 (offshore Angola): Biostratigraphy, paleoecology, and paleoceanographic significance: Journal of Foraminiferal Research, v. 43, p. 443–463, https://doi.org/10.2113/gsjfr.43.4.443.

Kochhann, K.G.D., Koutsoukos, E.A.M., and Fauth, G., 2014, Aptian–Albian benthic foraminifera from DSDP Site 364 (offshore Angola): A paleoenvironmental and paleobiogeographic appraisal: Cretaceous Research, v. 48, p. 1–11, https://doi.org/10.1016/j.cretres.2013.11.009.

Luft-Souza, F., Fauth, G., Bruno, M.D.R., De Lira Mota, M.A., Vázquez-García, B., Santos Filho, M.A.B., and Terra, G.J.S., 2022, Sergipe-Alagoas Basin, Northeast Brazil: A reference basin for studies on the early history of the South Atlantic Ocean: Earth-Science Reviews, v. 229, 104034, https://doi.org/10.1016/j.earscirev.2022.104034.

MacLeod, K.G., Martin, E.E., and Blair, S.W., 2008, Nd isotopic excursion across Cretaceous ocean anoxic event 2 (Cenomanian-Turonian) in the tropical North Atlantic: Geology, v. 36, p. 811–814, https://doi.org/10.1130/G24999A.1.

Martin, E.E., MacLeod, K.G., Jiménez Berrocoso, Á., and Bourbon, E., 2012, Water mass circulation on Demerara Rise during the Late Cretaceous based on Nd isotopes: Earth and Planetary Science Letters, v. 327–328, p. 111–120, https://doi.org/10.1016/j.epsl.2012.01.037.

Matsumoto, H., Coccioni, R., Frontalini, F., Shirai, K., Jovane, L., Trindade, R., Savian, J.F., and Kuroda, J., 2022, Mid-Cretaceous marine Os isotope evidence for heterogeneous cause of oceanic anoxic events: Nature Communications, v. 13, 239, https://doi.org/10.1038/s41467-021-27817-0.

McAnena, A., Flögel, S., Hofmann, P., Herrle, J.O., Griesand, A., Pross, J., Talbot, H.M., Rethemeyer, J., Wallmann, K., and Wagner, T., 2013, Atlantic cooling associated with a marine biotic crisis during the mid-Cretaceous period: Nature Geoscience, v. 6, p. 558–561, https://doi.org/10.1038/ngeo1850.

Müller, R.D., Mather, B., Dutkiewicz, A., Keller, T., Merdith, A., Gonzalez, C.M., Gorczyk, W., and Zahirovic, S., 2022, Evolution of Earth's tectonic carbon conveyor belt: Nature, v. 605, p. 629–639, https://doi.org/10.1038/s41586-022-04420-x.

Murphy, D.P., and Thomas, D.J., 2013, The evolution of Late Cretaceous deep-ocean circulation in the Atlantic basins: Neodymium isotope evidence from South Atlantic drill sites for tectonic controls: Geochemistry, Geophysics, Geosystems, v. 14, p. 5323–5340, https://doi.org/10.1002/2013GC004889.

O'Brien, C.L., et al., 2017, Cretaceous sea-surface temperature evolution: Constraints from TEX_{86} and planktonic foraminiferal oxygen isotopes: Earth-Science Reviews, v. 172, p. 224–247, https://doi.org/10.1016/j.earscirev.2017.07.012.

Pérez-Díaz, L., and Eagles, G., 2017, South Atlantic paleobathymetry since early Cretaceous: Scientific Reports, v. 7, 11819, https://doi.org/10.1038/s41598-017-11959-7.

Poulsen, C.J., Gendaszek, A.S., and Jacob, R.L., 2003, Did the rifting of the Atlantic Ocean cause the Cretaceous thermal maximum?: Geology, v. 31, p. 115–118, https://doi.org/10.1130/0091-7613(2003)031<0115:DTROTA>2.0.CO;2.

Pucéat, E., Lécuyer, C., and Reisberg, L., 2005, Neodymium isotope evolution of NW Tethyan upper ocean waters throughout the Cretaceous: Earth and Planetary Science Letters, v. 236, p. 705–720, https://doi.org/10.1016/j.epsl.2005.03.015.

Rahlf, P., Hathorne, E., Laukert, G., Gutjahr, M., Weldeab, S., and Frank, M., 2020, Tracing water mass mixing and continental inputs in the southeastern Atlantic Ocean with dissolved neodymium isotopes: Earth and Planetary Science Letters, v. 530, 115944, https://doi.org/10.1016/j.epsl.2019.115944.

Robinson, S.A., and Vance, D., 2012, Widespread and synchronous change in deep-ocean circulation in the North and South Atlantic during the Late Cretaceous: Paleoceanography, v. 27, PA1102, https://doi.org/10.1029/2011PA002240.

Robinson, S.A., Murphy, D.P., Vance, D., and Thomas, D.J., 2010, Formation of "Southern Component Water" in the Late Cretaceous: Evidence from Nd-isotopes: Geology, v. 38, p. 871–874, https://doi.org/10.1130/G31165.1.

Sanjinés, A.E.S., Viviers, M.C., Costa, D.S., dos Anjos Zerfass, G.S., Beurlen, G., and Strohschoen, O., Jr., 2022, Planktonic foraminifera from the Aptian section of the Southeastern Brazilian Atlantic margin: Cretaceous Research, v. 134, 105141, https://doi.org/10.1016/j.cretres.2022.105141.

Soudry, D., Glenn, C.R., Nathan, Y., Segal, I., and VonderHaar, D., 2006, Evolution of Tethyan phosphogenesis along the northern edges of the Arabian–African shield during the Cretaceous–Eocene as deduced from temporal variations of Ca and Nd isotopes and rates of P accumulation: Earth-Science Reviews, v. 78, p. 27–57, https://doi.org/10.1016/j.earscirev.2006.03.005.

Wagner, T., and Pletsch, T., 1999, Tectono-sedimentary controls on Cretaceous black shale deposition along the opening Equatorial Atlantic gateway (ODP Leg 159), *in* Cameron, N.R., et al., eds., The Oil and Gas Habitats of the South Atlantic: Geological Society, London, Special Publication 153, p. 241–265, https://doi.org/10.1144/GSL.SP.1999.153.01.15.

Printed in USA